



Published in final edited form as:

Curr Biol. 2010 December 7; 20(23): 2078–2089. doi:10.1016/j.cub.2010.10.008.

Meiotic Errors Activate Checkpoints that Improve Gamete Quality without Triggering Apoptosis in Male Germ Cells

Aimee Jaramillo-Lambert¹, Yuriko Harigaya^{2,3}, Jeffrey Vitt¹, Anne Villeneuve², and JoAnne Engebrecht^{1,*}

¹ Department of Molecular and Cellular Biology, Genetics Graduate Group, University of California, Davis, CA 95616

² Department of Developmental Biology, Stanford University School of Medicine, Stanford, California 94720

Summary

Background—Meiotic checkpoints ensure the production of gametes with the correct complement and integrity of DNA; in metazoans these pathways sense errors and transduce signals to trigger apoptosis to eliminate damaged germ cells. The extent to which checkpoints monitor and safeguard the genome differs between sexes and may contribute to the high frequency of human female meiotic errors. In the *C. elegans* female germ line, DNA damage, chromosome asynapsis and/or unrepaired meiotic double strand breaks (DSBs) activate checkpoints that induce apoptosis; conversely, male germ cells do not undergo apoptosis.

Results—Here we show that the recombination checkpoint is in fact activated in male germ cells despite the lack of apoptosis. The 9-1-1 complex and phosphatidylinositol 3-kinase-related protein kinase ATR, sensors of DNA damage, are recruited to chromatin in the presence of unrepaired meiotic DSBs in both female and male germ lines. Furthermore, checkpoint kinase CHK-1 is phosphorylated and p53 ortholog CEP-1 induces expression of BH3-only pro-apoptotic proteins in germ lines of both sexes under activating conditions. The core cell death machinery is expressed in female and male germ lines; however, CED-3 caspase is not activated in the male germ line. Although apoptosis is not triggered, checkpoint activation in males has functional consequences for gamete quality, as there is reduced viability of progeny sired by males with a checkpoint-activating defect in the absence of checkpoint function.

Conclusions—We propose that the recombination checkpoint functions in male germ cells to promote repair of meiotic recombination intermediates, thereby improving the fidelity of chromosome transmission in the absence of apoptosis.

Introduction

Eukaryotic organisms have surveillance mechanisms to monitor the integrity of the genome. When problems are encountered, such as DNA damage, these checkpoints halt the cell cycle and activate repair proteins to fix the damage. Alternatively, checkpoint activation can induce apoptosis to cull damaged cells [1]. During meiosis, several checkpoints function to ensure the fidelity of haploid gametes [2]. Some checkpoints, including the DNA damage

*Corresponding author: JoAnne Engebrecht, MCB, 1 Shields Ave; UC, Davis; Davis, CA. 95616.

³Current address: Department of Molecular and Cellular Biology, The University of Arizona Tucson, Arizona 85721

Publisher's Disclaimer: This is a PDF file of an unedited manuscript that has been accepted for publication. As a service to our customers we are providing this early version of the manuscript. The manuscript will undergo copyediting, typesetting, and review of the resulting proof before it is published in its final citable form. Please note that during the production process errors may be discovered which could affect the content, and all legal disclaimers that apply to the journal pertain.

checkpoint and a checkpoint to detect stalled replication, also function in somatic cells. Additionally, in meiosis checkpoints monitor recombination progression and chromosomal synapsis, features unique to meiotic prophase [2]. Failure in meiotic checkpoint control can lead to inviable or defective progeny.

Studies in many organisms have revealed that checkpoints comprise complex signaling networks, with different triggers and outputs involving both distinct and overlapping sets of components. Key factors of checkpoint pathways include sensors to detect errors/damage, transducers to transmit the signal, and effector proteins to elicit an appropriate biological response. The PCNA-like 9-1-1 complex (Rad9-Rad1-Hus1) is a sensor that localizes to chromatin in the presence of DNA damage or in response to unrepaired recombination intermediates [3,4]. The checkpoint signal is transduced through the PI(3)K (phosphatidylinositol-3-kinase) related protein kinases ATM (Ataxia-telangiectasia mutated) and ATR (Ataxia-telangiectasia mutated and rad3-related), which are thought to sense and respond to different types of lesions [5]. ATR and ATM amplify the checkpoint signal by phosphorylating multiple downstream targets, including the serine/threonine checkpoint kinases CHK1 and CHK2 [6]. Activation of CHK1 and CHK2 can delay cell cycle progression through inhibition of CDC25 or induce apoptotic removal of damaged cells via the tumor suppressor p53 [7,8].

In mammals, germline checkpoints appear to differ between the sexes. For example, mutants that fail to complete meiotic recombination (*e.g.* *Dmc1*^{-/-}, *Msh4*^{-/-} or *Msh5*^{-/-}) are sterile in both male and female mice [9–11]. However, while mouse oocytes progress to the pachytene sub-stage of meiotic prophase I before being removed by apoptosis, spermatocytes are eliminated earlier at late zygotene/early pachytene [11,12]. Meiotic germ cells that never initiate recombination (*e.g.* *Spo11*^{-/-} mutants) are also removed by apoptosis, which is triggered by a DNA-damage independent checkpoint that appears to be regulated differently in the sexes [13,14]. Finally, mutants defective in cell-cycle regulatory genes (*e.g.* *Cdk2*^{-/-}) also show sex-specific differences in checkpoint responses; male gametes arrest in early prophase I while female gametes progress to later stages [15]. Together, these phenotypes suggest that checkpoints are less stringent in the female germ line, a property that may partially explain the high degree of meiotic defects associated with female meiosis in humans [16].

The molecular basis underlying sex-specific differences in checkpoint function in mammals is not known, in part because of the greater technical difficulty in monitoring mammalian female meiosis compared with male meiosis. To investigate sex-specific checkpoint differences in a more tractable system, we utilized the unique features of the *C. elegans* reproductive system. *C. elegans* populations are composed predominantly of self-fertilizing hermaphrodites (XX), which as adults are genetically and structurally female, but males (X0) arise spontaneously at a low frequency (~0.2%) through chromosome nondisjunction. The germ lines of both sexes contain both mitotic and meiotic cells. In the distal most end of the gonad, proliferating germ cells serve as a stem cell population and are spatially separated from meiotic nuclei. Proximal to the proliferation zone, germ cells representing all stages of meiotic prophase are arranged in a spatial/temporal gradient along the distal to proximal axis (Figure 1A).

Several checkpoints operate in the *C. elegans* female germ line. Proliferating germ cells respond to perturbations by eliciting checkpoint-dependent cell cycle arrest [17]. In contrast, when meiotic germ cells are damaged or encounter errors, checkpoints trigger apoptosis [17,18]. The checkpoint pathways that respond to DNA damage and unrepaired recombination intermediates in female meiotic germ cells (Figure 2A) are conserved and activate the core apoptotic machinery [17]. Additionally, chromosome asynapsis is sensed

by a distinct checkpoint that requires PCH-2 [18]; the PCH-2 signaling pathway has not been elucidated. As in mammals, germline checkpoint function appears to differ between the *C. elegans* sexes. However, in this case, male germ cells do not induce apoptosis in response to DNA damage or chromosomal asynapsis [17,19], raising the possibility that checkpoints may be less stringent in the male germ line.

Here we investigate how the *C. elegans* male germ line responds to triggers that would elicit DNA damage/recombination checkpoint-induced apoptosis in the female germ line. We show that many checkpoint and apoptotic proteins are expressed and activated in the male germ line in response to DNA damage or meiotic errors. Further, apoptosis in male germ cells is blocked at the level of activation of the cell death machinery. Finally, we find that although the male germ line does not induce apoptosis in response to problems, checkpoint signaling nevertheless plays a critical role in gamete quality control, likely by ensuring the production of sperm with the correct genomic complement.

Results

DNA damage, chromosome asynapsis and/or unrepaired DSBs do not induce apoptosis in the male germ line

Some cells in the oogenic germ line of adult hermaphrodites undergo apoptosis under normal physiological conditions, while no apoptosis occurs in the spermatogenic germ line of males [20]. Nuclei in the pachytene region of the adult hermaphrodite germ line respond to perturbations by increasing the levels of apoptosis in a checkpoint-dependent manner [17]. Both physiological [20] and checkpoint-activated apoptosis [19] are dependent on oogenesis, and it has been reported that there is no apoptosis of male germ cells in response to ionizing radiation (IR) [17]. To confirm that nuclei in the male germ line do not undergo DNA damage-induced apoptosis, we examined wild-type hermaphrodite and male germ lines for apoptosis by Acridine Orange (AO) staining after exposure to IR (120 Gy). As expected, radiation resulted in increased levels of apoptosis in the hermaphrodite germ line compared to untreated worms (14.0 ± 0.9 vs. 2.5 ± 0.3 ; $p < 0.001$) (Figure 1B). The increased levels of apoptosis were checkpoint-dependent, as RNAi knockdown of the checkpoint kinase CHK-1 abrogated the IR-induced increase in apoptosis (Figure 1B). Following exposure to radiation, no apoptosis was observed in the male germ line (Figure 1B). To determine whether the male germ line could induce apoptosis in response to errors in meiosis, we examined hermaphrodite and male germ lines for apoptosis in mutants with chromosomal asynapsis and/or unrepaired recombination intermediates. SYP-1 is a central region component of the synaptonemal complex, and its loss results in asynapsis of all chromosome pairs and defects in recombination progression, activating both the recombination and synapsis checkpoint [21]. RAD-51 is a DNA strand exchange protein required for repair of DSBs, and *rad-51(RNAi)* results in a failure to repair breaks and activation of the recombination checkpoint [22]. Both the *syp-1(me17)* mutation and *rad-51(RNAi)* resulted in increased apoptosis (12.0 ± 0.5 and 5.2 ± 0.7 , respectively) in the hermaphrodite germ line, but no apoptosis was detected in the male germ line (Figure 1B).

AO fluoresces upon engulfment of apoptotic cells [20]. One possibility is that male germ cells undergo apoptosis but do not stain with AO because of lack of engulfment. To address this, we examined hermaphrodite and male germ lines for apoptosis by TUNEL labeling, which detects nuclei in the early DNA fragmentation step of the apoptotic program [23]. Wild-type hermaphrodite germ lines exposed to IR (120 Gy) had more TUNEL-positive nuclei than untreated controls (Figure 1C). No TUNEL positive nuclei were detected in the male germ line (Figure 1C). We also examined hermaphrodite and male germ lines of *nuc-1* mutants. NUC-1 is involved in DNA degradation during apoptosis; *nuc-1* mutants accumulate TUNEL-positive cells because they lack the major nuclease responsible for

elimination of fragmented DNA [24]. *nuc-1* hermaphrodites had many more TUNEL-positive nuclei after exposure to IR than untreated worms; however, no TUNEL-positive nuclei were detected in untreated or IR-exposed *nuc-1* male germ lines (Figure 1C). Thus, no detectable apoptosis is observed in the male germ line in response to DNA damage, chromosomal asynapsis, and/or unrepaired recombination intermediates.

Despite the lack of germline apoptosis in male pachytene cells, perturbation of S phase or exposure to IR resulted in arrest of nuclei within the proliferative zone of the male germ line, as in hermaphrodites [17] (Figure S1), suggesting that males are competent for checkpoint signaling.

The 9-1-1 complex protein HUS-1 localizes as distinct foci in both the hermaphrodite and male germ line in the presence of DNA damage and unrepaired DSBs

To determine if male meiotic germ cells sense DNA damage or recombination errors, we examined hermaphrodite and male germ lines under physiological and checkpoint-activating conditions for the localization of HUS-1, a component of the 9-1-1 DNA damage sensor complex, using worms expressing a HUS-1::GFP transgene [3]. In untreated, wild-type germ lines HUS-1::GFP is diffusely localized in pachytene nuclei in both hermaphrodites and males (Figure 2B). After exposure to IR, HUS-1::GFP localizes as distinct foci in pachytene nuclei of both hermaphrodites and males (Figure 2B). In *syp-1(RNAi)* treated worms HUS-1::GFP foci were observed in both hermaphrodite and male pachytene nuclei (Figure 2B). HUS-1 localization was also examined in *rad-51(RNAi)* and *zim-2(RNAi)* germ lines. ZIM-2 is a zinc finger protein that binds to chromosomal pairing centers, mediates chromosome pairing and also plays a role in detection of chromosomal asynapsis [25]. RNAi knock down of ZIM-2 results in asynapsis of chromosome V, causing defects in DSB repair and triggering the recombination checkpoint without activating the synapsis checkpoint. We observed HUS-1::GFP foci in pachytene nuclei of both *rad-51(RNAi)* and *zim-2(RNAi)* hermaphrodite and male germ lines (Figure 2B).

ATL-1 is recruited to chromatin in both male and hermaphrodite germ lines following DNA damage or in the presence of unrepaired DSBs

Following irradiation or in the presence of persistent DSBs, the checkpoint sensor ATR associates with chromatin to activate downstream target proteins (Figure 2A) [5]. In the hermaphrodite germ line, the ATR homolog, ATL-1, is recruited to chromatin following treatment with IR or when repair of meiotic DSBs is impaired [26]. To ascertain whether ATL-1 functions as a checkpoint sensor in the male germ line, we monitored recruitment of ATL-1 by immunofluorescence after IR and in recombination-defective mutants [*rad-51(RNAi)*, *syp-1(me17)*, and *zim-2(tm574)*]. Following IR treatment, ATL-1 foci accumulate in pachytene nuclei in both hermaphrodite and male germ lines (Figure 2C). ATL-1 foci were also detected in pachytene nuclei of *syp-1(me17)* and *zim-2(tm574)* hermaphrodites and males and in worms depleted of RAD-51 (Figure 2C). These data reveal that ATL-1 can sense DNA damage and unrepaired recombination intermediates in the male germ line as it does in the hermaphrodite germ line.

CHK-1 is phosphorylated in the germ line of both sexes upon checkpoint activation

The DNA damage and unrepaired recombination checkpoint signal is relayed through ATR-directed phosphorylation at Ser345 of the checkpoint kinase CHK-1, which in turn activates downstream effectors of the checkpoint signaling pathway (Figure 2A) [6]. To determine if CHK-1 was expressed in the male germ line, we performed immunofluorescence using an antibody that recognizes the full-length protein. CHK-1 showed a nucleoplasm staining pattern in pachytene nuclei of both hermaphrodites and males that was greatly reduced in *chk-1(RNAi)* treated worms (Figure 3A). To determine if CHK-1 is activated in response to

DNA damage or errors in meiosis, we examined the phosphorylation status of CHK-1 in both hermaphrodite and male germ lines using an antibody against phospho-Ser345 of CHK-1 (PO₄-CHK-1). Faint PO₄-CHK-1 foci were detected in untreated germ lines of both hermaphrodites and males (Figure 3B). Following IR treatment and in the recombination defective mutants [*syp-1(me17)* and *zim-1(tm1813)*], PO₄-CHK-1 localized as intense foci in pachytene nuclei of hermaphrodites and males (Figure 3B). ZIM-1 is another zinc finger protein that binds to chromosome II and III pairing centers and mediates their pairing; the *zim-1(tm1813)* mutant results in asynapsis of these chromosomes, causing defects in DSB repair and triggering the recombination checkpoint without activating the synapsis checkpoint [25]. In both hermaphrodite and male *chk-1(RNAi)* germ lines staining was largely eliminated (Figure 3B). CHK-1 phosphorylation following IR treatment and in the presence of unrepaired meiotic DSBs [*zim-2(tm574)*] was also confirmed by immunoblotting of hermaphrodite and male worm extracts with the pSer345 CHK1 antibody (Figure 3C). Taken together, these data indicate that CHK-1 is expressed in the male germ line and phosphorylated under checkpoint-activating conditions as it is in hermaphrodites.

CEP-1(p53) is expressed and induces *egl-1* expression in response to DNA damage and unrepaired DSBs in both the hermaphrodite and male germ line

In the hermaphrodite germ line, the CEP-1(p53) transcription factor is required for germline apoptosis in response to DNA damage, and in mammalian systems p53 functions downstream of CHK1 [27,28]. Previous analysis indicated that CEP-1 was expressed in the proliferative zone of males [29]; to determine whether CEP-1 is also expressed in the male germ line during meiotic prophase, we used a CEP-1-specific antibody. In the hermaphrodite germ line, CEP-1 is found in nuclei from late pachytene through the diplotene stage (Figure 4A) [30]. CEP-1 also localizes to the nucleoplasm in late pachytene nuclei of the male germ line, and as expected, CEP-1 staining is completely abrogated in *cep-1(gk138)* germ lines (Figure 4A). No change in CEP-1 localization or staining intensity was observed under checkpoint-activating conditions in either hermaphrodite or male germ lines (Figure S2A) [30].

In the *C. elegans* hermaphrodite germ line, the pro-apoptotic BH3-only domain containing protein EGL-1 is a transcriptional target of CEP-1 [3]. We analyzed *egl-1* expression in hermaphrodites and males by quantitative real-time PCR (qRT-PCR) from whole worm extracts before and after exposure to IR (120 Gy). As previously reported [3], the level of *egl-1* transcript was increased in hermaphrodites exposed to IR (Figure 4B). *egl-1* steady state transcript levels were also increased in a *cep-1*-dependent manner in males exposed to IR (Figure 4B). To determine if the transcriptional induction of *egl-1* was occurring in meiotic germ cells, we examined *egl-1* transcript levels in *zim-1(tm1813)* worms. *zim-1* is expressed and functions predominantly in the germ line of adult worms [25,31]. Furthermore, the checkpoint-triggering defect in *zim-1* mutants is specific to meiotic prophase, as the *zim-1* mutation did not elicit cell cycle arrest in the proliferating region of the germ lines of either hermaphrodites or males (Figure S1). *egl-1* steady state transcript levels were significantly increased in both *zim-1(tm1813)* hermaphrodites and males relative to wild-type controls, suggesting that *egl-1* induction is occurring in meiotic prophase germ cells (Figure 4B). To determine if *egl-1* induction in the *zim-1* mutant was checkpoint-dependent, we performed qRT-PCR with RNA isolated from *zim-1(tm1813);cep-1(RNAi)* and *zim-1(tm1813);chk-1(RNAi)* hermaphrodites and males. Steady-state *egl-1* RNA levels were greatly reduced in both *zim-1(tm1813);cep-1(RNAi)* hermaphrodites and males relative to mock RNAi treated controls (*zim-1* L4440) (Figure 4C). Induction of *egl-1* transcripts was reduced but not completely eliminated in *zim-1;chk-1(RNAi)* hermaphrodites and males (Figure 4C). RNAi feeding of *chk-1* was efficient as *chk-1* transcripts were reduced relative to mock RNAi-treated worms (Figure S2B). In addition, *ced-13*, a second *C. elegans* BH3-

only domain protein and CEP-1(p53) target [32], was induced in response to DNA damage and unrepaired recombination intermediates in hermaphrodites and males (Figure S2C). Taken together, these data suggest that both DNA damage and unrepaired recombination intermediates induce CEP-1-dependent transcription of BH3-only domain proteins in the male germ line.

The apoptotic machinery is expressed but CED-3 caspase is not activated in the male germ line

In *C. elegans*, EGL-1 activates apoptosis by binding anti-apoptotic protein CED-9 (Bcl-2), causing a conformational change and release of the protease activator CED-4 (Apaf-1) from the mitochondrial membrane [33,34]. Once released, CED-4 translocates to the nuclear membrane and oligomerizes, bringing two CED-3 caspases into close proximity for self-activation (Figure 5A) [34]. Because *egl-1* is transcriptionally-induced in the male germ line in response to DNA damage and unrepaired recombination intermediates but no apoptosis is observed, we examined the status of the core apoptotic machinery in hermaphrodite and male germ lines. To that end, we monitored apoptosis in the *ced-9(n1653)* temperature sensitive allele. At the permissive temperature (15°C), hermaphrodites had low levels of apoptosis by AO staining, and no apoptotic nuclei were detected in male germ lines (Figure 5B). At the nonpermissive temperature (25°C), the number of apoptotic nuclei increased in hermaphrodite, but not male, germ lines (Figure 5B). This was also true under checkpoint-activating conditions (IR, 120 Gy) (Figure 5B). TUNEL labeling in *nuc-1;ced-9(RNAi)* germ lines confirmed these results: *nuc-1;ced-9(RNAi)* hermaphrodites had on average 2 TUNEL positive nuclei/gonad but this dramatically increased to greater than 14 TUNEL positive nuclei/gonad following IR exposure; no TUNEL-positive nuclei were detected in male *nuc-1;ced-9(RNAi)* germ lines exposed to IR (n=9 gonads). These data suggest that apoptosis is blocked in the male germ line downstream of CED-9.

We next examined germ lines for expression and localization of CED-4. In hermaphrodite germ lines CED-4 localized to the nuclear periphery of meiotic prophase nuclei (Figure 5C) [35]. CED-4 was also expressed and localized to the nuclear periphery of pachytene cells in male germ lines (Figure 5C); staining was absent in *ced-4(RNAi)* worms (Figure S3A). As has been previously reported [35], we observed an occasional nucleus with more intense staining in both hermaphrodite and male germ lines (Figure 5C, arrowheads).

SIR-2.1, a *C. elegans* member of the Sirtuin family of NAD⁺-dependent protein deacetylases, is required for DNA damage-induced germline apoptosis [35]. Sir-2.1 translocates from the nucleus to the cytoplasm where it has been proposed to interact with CED-4 to promote apoptosis [35]. SIR-2.1 was observed in germ cell nuclei in both hermaphrodites and males (Figure 5C), but not in the *sir-2.1(ok434)* mutant (Figure S3B). However, unlike in hermaphrodites, SIR-2.1 remained in all male germ cell nuclei even in *zim-1* mutants (Figure 5C). Thus, SIR-2.1 does not undergo translocation out of the nucleus in male germ cells.

Finally, we analyzed the expression and localization of the cell death executor caspase CED-3. CED-3 was observed around pachytene germ cell nuclei in both hermaphrodites and males (Figure 5D). However, upon checkpoint activation in *syp-1(me17)* and *zim-1(tm1813)* mutant hermaphrodites, CED-3 foci were more intense (Figure 5D). Interestingly, we noted that CED-3 foci did not localize around nuclei containing the highly condensed chromatin characteristic of late stage apoptosis in *syp-1(me17)* and *zim-1(tm1813)* hermaphrodites (Figure 5, arrowheads). In contrast to the hermaphrodite germ line, there was no noticeable change in the intensity or localization of CED-3 upon checkpoint activation in pachytene nuclei of males (Figure 5D).

Caspases exist as proenzymes that become active upon proteolytic cleavage. To qualitatively measure caspase activity in the germ line, a cell-permeant fluorescent caspase inhibitor (SR-FLICA) was injected into germ lines of hermaphrodites and males. Active caspase covalently binds the FLICA inhibitor, resulting in fluorescent cells [36] and was detected as a fluorescent signal that encircled apoptotic nuclei. While very few fluorescent cells were found in wild-type hermaphrodite germ lines (fluorescent cells were not detected in every gonad), none were found in wild-type male germ lines ($n = 20$; Figure 5E). To examine caspase activity in response to checkpoint signaling, the fluorescent caspase inhibitor was injected into *zim-1(tm1813)* hermaphrodites and males. Caspase-positive cells were detected in *zim-1* hermaphrodite germ lines, and these were eliminated by treatment with *ced-3(RNAi)* (Figure 5E). Caspase activity was not detected in *zim-1* male germ lines ($n = 36$; Figure 5E), suggesting that caspase is not activated in the male germ line.

The recombination checkpoint functions in the male germ line to enhance gamete quality when meiosis is impaired

Our analyses have revealed that both hermaphrodite and male germ lines sense DNA damage and unrepaired meiotic breaks and activate checkpoint signaling, but checkpoint activation does not lead to apoptosis in the male germ line due to a block at the level of the cell death machinery. In hermaphrodites, a similar block to apoptosis under checkpoint-activating conditions results in increased meiotic non-disjunction [18,25], implying that checkpoint-triggered apoptosis serves as a culling mechanism to eliminate germ cells with high levels of unrepaired DSBs. Thus, one might anticipate that a consequence of the lack of this culling mechanism in males would be that sperm from mutants with checkpoint-activating meiotic defects should cause a higher frequency of progeny lethality than their oocyte counterparts. We tested this hypothesis by evaluating the relative levels of progeny inviability conferred by *zim-2(tm574)* and *zim-1(tm1813)* mutant sperm and ova. Both hermaphrodite [25] and male *zim-2* mutant germ cells have one asynapsed chromosome pair (Figure S4A), and both exhibited checkpoint activation in our prior assays (Figures 2B, C, 3C). *zim-1* mutant germ cells have two asynapsed chromosome pairs [40], and also exhibited checkpoint activation in hermaphrodites and males (Figures 3B,4B, C). For these experiments, we used the *fog-2* mutation to eliminate hermaphrodite spermatogenesis, rendering XX animals female [37] so that the contribution of each parent to progeny lethality could be assessed unambiguously. As expected, when meiosis was unperturbed, there was excellent progeny viability (WT: 0.66% inviable progeny); conversely, when both parents were mutant for either *zim-2* or *zim-1*, progeny viability was significantly impaired (*zim-2*: 34.7%; *zim-1*: 73.2% inviable progeny) (Figure 6A). Contrary to the prediction of the above hypothesis, when *zim-2* or *zim-1* sperm fertilized *fog-2* oocytes, there was significantly better progeny viability (*zim-2*: 13.7%; *zim-1*: 24.9% inviable progeny) than when *zim-2*; *fog-2* or *zim-1*; *fog-2* oocytes were fertilized by wild-type sperm (*zim-2*: 23.4%; *zim-1*: 47% inviable progeny) (Figure 6A), even though female germ cells are culled by apoptosis but male germ cells are not. Thus, the absence of germ cell culling by checkpoint-activated apoptosis in the male germ line does not result in reduced gamete quality relative to that of the female germ line.

The relatively high viability of progeny sired by *zim-2* and *zim-1* males suggested that checkpoint activation in males may improve gamete quality. To test this hypothesis, we monitored the consequences of inactivating components of the recombination checkpoint signaling pathway in *zim-2* and *zim-1* males. As shown in Figure 6B, progeny viability was significantly impaired when ATL-1 was depleted in *zim-2(tm574)* and *zim-1(tm1813)* males (*zim-2*: 24.3 vs. 10.3% inviable progeny, $p < 0.0001$; *zim-1*: 43.8 vs. 24.9% inviable progeny, $p < 0.0001$) but not in otherwise wild-type males (*atl-1*: 3.1% vs. wt: 1.9% inviable progeny). Similarly, we found that progeny sired by *atl-1(tm583)* mutant males had reduced viability

that was exacerbated by RNAi depletion of *zim-2* or *zim-1* (Figure S4B). We also examined viability of progeny sired by 9-1-1 complex *hus-1(op241)* mutant males; *hus-1(op241)* is a hypomorphic allele [3]. As with *atl-1(tm583)*, depletion of *zim-2* and *zim-1* by RNAi resulted in enhanced progeny inviability in *hus-1(op241)* males (Figure S4B). In contrast to *atl-1* and *hus-1*, depletion of *cep-1*, which induces the apoptotic pathway in the female germ line, did not enhance progeny inviability in the absence of *zim-2* or *zim-1*, suggesting that CEP-1 does not contribute to improved sperm quality (Figure 6B). Thus, although checkpoint signaling does not induce apoptosis in the male germ line, the checkpoint does play an important role in enhancing sperm quality, presumably by helping to ensure that sperm have an appropriate and intact DNA complement.

To determine if the checkpoint facilitated repair of DSBs, we monitored the appearance and disappearance of RAD-51 foci in *zim-1(tm1813)* hermaphrodite and male germ lines in the presence and absence of the recombination checkpoint. In *zim-1* hermaphrodite germ lines there was an apparent global increase in the number of DSBs as well as a persistence of breaks into late stages of pachytene, as has been observed in other chromosomal asynapsis mutants [38], and this was not altered in the absence of the checkpoint (Figure 6C). In contrast, males had on average more RAD-51 foci at earlier stages of meiotic prophase, and this was further enhanced in the absence of the checkpoint (Figure 6C). We also noticed that there were fewer crescent-shaped nuclei in the transition zone in *zim-1* mutant males, but not hermaphrodites, when ATL-1 was depleted (*zim-1* males: 30 ± 7 ; *zim-1; atl-1* males: 18 ± 3 ; $p < 0.001$). These results suggest that the recombination checkpoint regulates DSB repair and meiotic progression in the male germ line.

Discussion

Our analyses of checkpoint signaling in the *C. elegans* male germ line revealed that the checkpoint and apoptotic machinery are largely expressed and can be activated in males, but no apoptosis occurs. Nonetheless, we show that checkpoint activation is functionally important during male meiosis. Males are apparently even more successful at handling an asynapsed chromosome pair during meiosis than are hermaphrodites, and improved success of chromosome transmission depends on the checkpoint machinery. Thus, checkpoints appear to be more successful during spermatocyte meiosis than oocyte meiosis in ensuring the production of haploid gametes with the correct complement of DNA.

Absence of apoptosis in the male germ line

Surprisingly, we discovered that the checkpoint signaling cascade is activated and the core death machinery is expressed in the male germ line, although no apoptosis occurs. The absence of apoptosis is likely because of the failure of the executor of death, CED-3 caspase to be activated. This may be due to direct inhibition of caspase, or indirectly through other components of the apoptotic machinery, perhaps mediated by the protein deacetylase SIR-2.1. The mechanism underlying SIR-2.1 function in DNA damage-induced germline apoptosis is unknown, although it correlates with translocation of SIR-2.1 out of the nucleus [35]. We found that while SIR-2.1 is expressed in male germline nuclei, it does not translocate. It has been suggested that as SIR-2.1 translocates it interacts with CED-4 to promote apoptosis [35]; however, SIR-2.1 could mediate apoptosis through interaction with other components of the cell death machinery such as CED-3, a caspase inhibitor, or other proteins. Nonetheless, CED-3 is not activated in the male germline as levels of CED-3 do not increase as in hermaphrodites following checkpoint induction and using a fluorescent inhibitor, no active caspase activity was detected. Regulation of caspase activity via inhibitors is a widely used mechanism to control apoptosis [39]. While there are caspase inhibitors in *C. elegans*, none have been found that are expressed in the male germ line

[40,41]. Future work may shed light on the mechanism underlying inhibition of the cell death machinery in the *C. elegans* male germ line.

Additional features of the male gonad might also contribute to blocking apoptosis. Phagocytosis of apoptotic cells has been shown to promote death [42,43]. In hermaphrodite germ lines apoptotic nuclei are rapidly phagocytosed by the surrounding somatic sheath cells [20], which are not present in males. However, the absence of sheath cells can not solely explain the lack of apoptosis as *fog-1*, which has an oogenic germ line but a male soma and lacks sheath cells, is competent for apoptosis [19,20]. Germ cell apoptosis also requires MAP kinase activation [20,44]. In adult males, MPK-1 is expressed and activated in the distal germ line, but is absent from pachytene nuclei [45]. In hermaphrodites, apoptosis can occur in the absence of MAPK signaling when CED-9 is also inactivated [20]. As inactivation of CED-9 in males did not result in apoptosis (Figure 5B), it is unlikely that the absence of MPK-1 in the pachytene region of the male germ line in and of itself blocks apoptosis. Taken together, apoptosis in the male germ line appears to be prevented predominantly by inhibition of the cell death machinery, with the lack of sheath cells and MAPK potentially playing ancillary roles.

Pro-apoptotic gene expression and the absence of apoptosis

DNA damage induces a checkpoint-dependent cell cycle arrest in germ cells of the proliferative zone in hermaphrodite and male germ lines [17] (Figure S1). Unlike the checkpoint response in mammals, cell cycle arrest in response to IR-induced damage in *C. elegans* germ cells is not dependent on CEP-1(p53) [27]. In meiotic germ cells, DNA damage and meiotic errors induce the CEP-1-dependent transcription of the pro-apoptotic gene *egl-1* (this study, [3]). Interestingly, *egl-1* is also expressed in proliferating nuclei in response to IR, even though these nuclei are not competent for apoptosis [3,17]. Similarly to *cep-1*, cell cycle arrest is not dependent on *egl-1* [46]. Why is *cep-1* activated and *egl-1* transcriptionally-induced in the proliferative zone and in male germ lines when no apoptosis occurs? One possibility is that checkpoint activation does not discriminate between downstream effectors of the signaling pathway, and thus activation signals through *cep-1* and induces expression of pro-apoptotic genes even when apoptosis is blocked. Alternatively, these proteins may have additional roles in the germ line. In support of this, a recent study found that meiotic recombination normally induces p53 activation in *Drosophila* [47].

The role of checkpoint signaling in the male germ line

We have shown that checkpoint pathway components are recruited to chromatin in response to DNA damage or perturbations in meiosis in the male germ line. Even though male germ cells are not eliminated through apoptosis when checkpoints are activated, checkpoint proteins nevertheless play an important role in promoting gamete success. This was directly demonstrated by the fact that abrogation of checkpoint function significantly elevated the frequency of inviable progeny sired by males with a checkpoint-activating defect in meiotic chromosome synapsis. How does checkpoint activation in the male germ line improve reproductive success? Apoptosis is only one potential output of checkpoint signaling; in addition, checkpoint pathways can control the cell cycle and/or activate repair pathways. We observed no difference in the overall duration of male meiotic prophase in the presence of checkpoint activation suggesting that the checkpoint does not induce arrest (unpublished data) [17], although fewer crescent-shaped nuclei were observed in the transition zone in the absence of the checkpoint. The more abundant and earlier appearance of RAD-51 foci suggests that the recombination checkpoint plays a role in enhancing the efficiency of DNA repair. This could potentially involve transcriptional upregulation and activation of genes whose products are involved in DNA repair, as occurs in yeast and mammalian cells [1,48].

Alternatively, or in addition, enhancement of repair could involve more efficient recruitment of repair proteins to sites where their activities are needed. The end result would be to minimize the likelihood of unrepaired breaks being present in gametes and transmitted to progeny, consequently impairing progeny viability.

In the course of our experiments, we discovered that male spermatocytes are actually more successful than oocytes at handling the consequences of an asynapsed chromosome pair(s). This likely reflects operation of a mechanism for segregation of achiasmate chromosomes that may be absent or ineffectual in oocyte meiosis. Achiasmate segregation mechanisms are well established in *Drosophila*, and there is also evidence for such mechanisms in yeast and other eukaryotes [49,50]. Sex differences in the ability to segregate achiasmate chromosomes may be attributed to males having a constitutively asynaptic X chromosome, differences in the organization of chromosomes within nuclei at the end of meiotic prophase [51] and/or differences in the organization and assembly of meiotic spindles [52]. An ability of spermatocytes to correctly segregate an achiasmate chromosome pair may act in parallel with enhanced efficiency of repair in response to checkpoint activation to minimize the consequences of meiotic prophase errors during spermatogenesis. Alternatively, rather than representing two distinct quality control mechanisms, it is possible that checkpoint activation itself might induce the achiasmate segregation mechanism.

Concluding remarks—We have shown that checkpoints operate in distinct ways in the *C. elegans* female and male germ lines, in the case of oogenesis, using apoptosis to prevent defective germ cells from becoming gametes, and in the case of spermatogenesis, by improving the quality of the gametes produced. Our findings emphasize the fact that even within a single species, diverse quality control strategies can be used to achieve the same end, i.e., ensuring the faithful transmission of the genome from generation to generation.

Experimental Procedures

Standard methods were used for worm genetics, RNAi, quantification of germline apoptosis, immunostaining, and quantitative RT-PCR. Detailed methods are described in supplementary materials.

Caspase Assay

Adult worms 16h post-L4 larval stage were microinjected with a 30X dilution of SulfoRhodamine-Fluorescent-Labeled Inhibitor of CASpases (SR-FLICA) poly-caspase reagent (Immunochemistry Technologies, Bloomington, MN). Immediately following injection worms were recovered in M9 buffer and transferred to a fresh NGM plate and incubated in the dark for 1h. Worms were mounted under coverslips in M9 on 3% agarose pads containing 0.2mM tetramisole. Caspase activity was determined by fluorescence microscopy and DIC using a Zeiss Axioskop 2. A minimum of 20 gonads was examined for each genotype.

Supplementary Material

Refer to Web version on PubMed Central for supplementary material.

Acknowledgments

We thank S. Boulton, A. Gartner, and A. La Volpe for generously providing antibodies. We also thank the *Caenorhabditis* Genetics Center for strains and P. Checchi, W.D. Heyer, K. Lawrence and L. Rose for helpful discussions and comments on the manuscript. This work was supported by National Institutes of Health (NIH) GM086505 and the Agricultural Experimental Station CA-D*MCB-7237-H to J.E. and NIH R01 GM067268 to

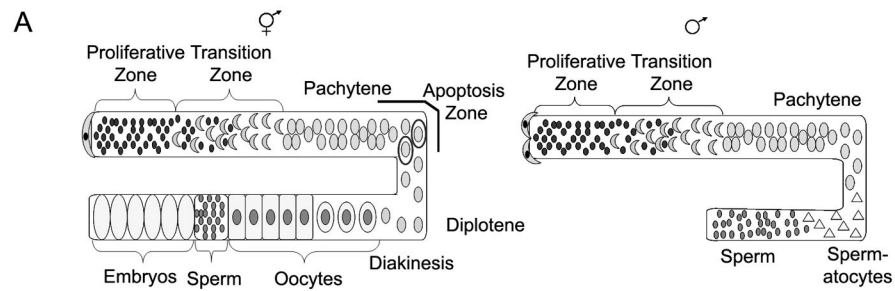
A.V. A.J.L. was supported by NIH T32GM070377 and a University of California, Davis Office of Graduate Studies Dissertation Year Fellowship.

Literature Cited

1. Zhou BB, Elledge SJ. The DNA damage response: putting checkpoints in perspective. *Nature*. 2000; 408:433–439. [PubMed: 11100718]
2. Hochwagen A, Amon A. Checking your breaks: surveillance mechanisms of meiotic recombination. *Curr Biol*. 2006; 16:R217–228. [PubMed: 16546077]
3. Hofmann ER, Milstein S, Boulton SJ, Ye M, Hofmann JJ, Stergiou L, Gartner A, Vidal M, Hengartner MO. *Caenorhabditis elegans* HUS-1 is a DNA damage checkpoint protein required for genome stability and EGL-1-mediated apoptosis. *Curr Biol*. 2002; 12:1908–1918. [PubMed: 12445383]
4. Volkmer E, Karnitz LM. Human homologs of *Schizosaccharomyces pombe* rad1, hus1, and rad9 form a DNA damage-responsive protein complex. *J Biol Chem*. 1999; 274:567–570. [PubMed: 9872989]
5. Abraham RT. Cell cycle checkpoint signaling through the ATM and ATR kinases. *Genes Dev*. 2001; 15:2177–2196. [PubMed: 11544175]
6. Nojima H. Protein kinases that regulate chromosome stability and their downstream targets. *Genome Dyn*. 2006; 1:131–148. [PubMed: 18724058]
7. Furnari B, Blasina A, Boddy MN, McGowan CH, Russell P. Cdc25 inhibited in vivo and in vitro by checkpoint kinases Cds1 and Chk1. *Mol Biol Cell*. 1999; 10:833–845. [PubMed: 10198041]
8. Levine AJ. p53, the cellular gatekeeper for growth and division. *Cell*. 1997; 88:323–331. [PubMed: 9039259]
9. Edelmann W, Cohen PE, Kneitz B, Winand N, Lia M, Heyer J, Kolodner R, Pollard JW, Kucherlapati R. Mammalian MutS homologue 5 is required for chromosome pairing in meiosis. *Nat Genet*. 1999; 21:123–127. [PubMed: 9916805]
10. Kneitz B, Cohen PE, Avdievich E, Zhu L, Kane MF, Hou H Jr, Kolodner RD, Kucherlapati R, Pollard JW, Edelmann W. MutS homolog 4 localization to meiotic chromosomes is required for chromosome pairing during meiosis in male and female mice. *Genes Dev*. 2000; 14:1085–1097. [PubMed: 10809667]
11. Pittman DL, Cobb J, Schimenti KJ, Wilson LA, Cooper DM, Brignull E, Handel MA, Schimenti JC. Meiotic prophase arrest with failure of chromosome synapsis in mice deficient for Dmc1, a germline-specific RecA homolog. *Mol Cell*. 1998; 1:697–705. [PubMed: 9660953]
12. Cohen PE, Pollack SE, Pollard JW. Genetic analysis of chromosome pairing, recombination, and cell cycle control during first meiotic prophase in mammals. *Endocr Rev*. 2006; 27:398–426. [PubMed: 16543383]
13. Baudat F, Manova K, Yuen JP, Jasin M, Keeney S. Chromosome synapsis defects and sexually dimorphic meiotic progression in mice lacking Spo11. *Mol Cell*. 2000; 6:989–998. [PubMed: 11106739]
14. Romanienko PJ, Camerini-Otero RD. The mouse Spo11 gene is required for meiotic chromosome synapsis. *Mol Cell*. 2000; 6:975–987. [PubMed: 11106738]
15. Ortega S, Prieto I, Odajima J, Martin A, Dubus P, Sotillo R, Barbero JL, Malumbres M, Barbacid M. Cyclin-dependent kinase 2 is essential for meiosis but not for mitotic cell division in mice. *Nat Genet*. 2003; 35:25–31. [PubMed: 12923533]
16. Hassold T, Hunt P. To err (meiotically) is human: the genesis of human aneuploidy. *Nat Rev Genet*. 2001; 2:280–291. [PubMed: 11283700]
17. Gartner A, Milstein S, Ahmed S, Hodgkin J, Hengartner MO. A conserved checkpoint pathway mediates DNA damage--induced apoptosis and cell cycle arrest in *C. elegans*. *Mol Cell*. 2000; 5:435–443. [PubMed: 10882129]
18. Bhalla N, Dernburg AF. A conserved checkpoint monitors meiotic chromosome synapsis in *Caenorhabditis elegans*. *Science*. 2005; 310:1683–1686. [PubMed: 16339446]

19. Jaramillo-Lambert A, Engebrecht J. A single unpaired and transcriptionally silenced X chromosome locally precludes checkpoint signaling in the *Caenorhabditis elegans* germ line. *Genetics*. 2010; 184:613–628. [PubMed: 20008570]
20. Gumienny TL, Lambie E, Hartweg E, Horvitz HR, Hengartner MO. Genetic control of programmed cell death in the *Caenorhabditis elegans* hermaphrodite germline. *Development*. 1999; 126:1011–1022. [PubMed: 9927601]
21. MacQueen AJ, Colaiacovo MP, McDonald K, Villeneuve AM. Synapsis-dependent and -independent mechanisms stabilize homolog pairing during meiotic prophase in *C. elegans*. *Genes Dev*. 2002; 16:2428–2442. [PubMed: 12231631]
22. Alpi A, Pasierbek P, Gartner A, Loidl J. Genetic and cytological characterization of the recombination protein RAD-51 in *Caenorhabditis elegans*. *Chromosoma*. 2003; 112:6–16. [PubMed: 12684824]
23. Gavrieli Y, Sherman Y, Ben-Sasson SA. Identification of programmed cell death in situ via specific labeling of nuclear DNA fragmentation. *J Cell Biol*. 1992; 119:493–501. [PubMed: 1400587]
24. Wu YC, Stanfield GM, Horvitz HR. NUC-1, a *Caenorhabditis elegans* DNase II homolog, functions in an intermediate step of DNA degradation during apoptosis. *Genes Dev*. 2000; 14:536–548. [PubMed: 10716942]
25. Phillips CM, Dernburg AF. A family of zinc-finger proteins is required for chromosome-specific pairing and synapsis during meiosis in *C. elegans*. *Dev Cell*. 2006; 11:817–829. [PubMed: 17141157]
26. Garcia-Muse T, Boulton SJ. Distinct modes of ATR activation after replication stress and DNA double-strand breaks in *Caenorhabditis elegans*. *Embo J*. 2005; 24:4345–4355. [PubMed: 16319925]
27. Schumacher B, Hofmann K, Boulton S, Gartner A. The *C. elegans* homolog of the p53 tumor suppressor is required for DNA damage-induced apoptosis. *Curr Biol*. 2001; 11:1722–1727. [PubMed: 11696333]
28. Shieh SY, Ahn J, Tamai K, Taya Y, Prives C. The human homologs of checkpoint kinases Chk1 and Cds1 (Chk2) phosphorylate p53 at multiple DNA damage-inducible sites. *Genes Dev*. 2000; 14:289–300. [PubMed: 10673501]
29. Gao MX, Liao EH, Yu B, Wang Y, Zhen M, Derry WB. The SCF FSN-1 ubiquitin ligase controls germline apoptosis through CEP-1/p53 in *C. elegans*. *Cell Death Differ*. 2008; 15:1054–1062. [PubMed: 18340346]
30. Schumacher B, Hanazawa M, Lee MH, Nayak S, Volkmann K, Hofmann ER, Hengartner M, Schedl T, Gartner A. Translational repression of *C. elegans* p53 by GLD-1 regulates DNA damage-induced apoptosis. *Cell*. 2005; 120:357–368. [PubMed: 15707894]
31. Reinke V, Smith HE, Nance J, Wang J, Van Doren C, Begley R, Jones SJ, Davis EB, Scherer S, Ward S, et al. A global profile of germline gene expression in *C. elegans*. *Mol Cell*. 2000; 6:605–616. [PubMed: 11030340]
32. Schumacher B, Schertel C, Wittenburg N, Tuck S, Mitani S, Gartner A, Conradt B, Shaham S. *C. elegans ced-13* can promote apoptosis and is induced in response to DNA damage. *Cell Death Differ*. 2005; 12:153–161. [PubMed: 15605074]
33. Conradt B, Horvitz HR. The *C. elegans* protein EGL-1 is required for programmed cell death and interacts with the Bcl-2-like protein CED-9. *Cell*. 1998; 93:519–529. [PubMed: 9604928]
34. del Peso L, Gonzalez VM, Nunez G. *Caenorhabditis elegans* EGL-1 disrupts the interaction of CED-9 with CED-4 and promotes CED-3 activation. *J Biol Chem*. 1998; 273:33495–33500. [PubMed: 9837929]
35. Greiss S, Hall J, Ahmed S, Gartner A. *C. elegans* SIR-2.1 translocation is linked to a proapoptotic pathway parallel to cep-1/p53 during DNA damage-induced apoptosis. *Genes Dev*. 2008; 22:2831–2842. [PubMed: 18923081]
36. Lee BW, Olin MR, Johnson GL, Griffin RJ. In vitro and in vivo apoptosis detection using membrane permeant fluorescent-labeled inhibitors of caspases. *Methods Mol Biol*. 2008; 414:109–135. [PubMed: 18175816]

37. Schedl T, Kimble J. *fog-2*, a germ-line-specific sex determination gene required for hermaphrodite spermatogenesis in *Caenorhabditis elegans*. *Genetics*. 1988; 119:43–61. [PubMed: 3396865]
38. Carlton PM, Farruggio AP, Dernburg AF. A link between meiotic prophase progression and crossover control. *PLoS Genet*. 2006; 2:e12. [PubMed: 16462941]
39. O’Riordan MX, Bauler LD, Scott FL, Duckett CS. Inhibitor of apoptosis proteins in eukaryotic evolution and development: a model of thematic conservation. *Dev Cell*. 2008; 15:497–508. [PubMed: 18854135]
40. Geng X, Shi Y, Nakagawa A, Yoshina S, Mitani S, Shi Y, Xue D. Inhibition of CED-3 zymogen activation and apoptosis in *Caenorhabditis elegans* by caspase homolog CSP-3. *Nat Struct Mol Biol*. 2008; 15:1094–1101. [PubMed: 18776901]
41. Geng X, Zhou QH, Kage-Nakadai E, Shi Y, Yan N, Mitani S, Xue D. *Caenorhabditis elegans* caspase homolog CSP-2 inhibits CED-3 autoactivation and apoptosis in germ cells. *Cell Death Differ*. 2009; 16:1385–1394. [PubMed: 19575016]
42. Hoepfner DJ, Hengartner MO, Schnabel R. Engulfment genes cooperate with *ced-3* to promote cell death in *Caenorhabditis elegans*. *Nature*. 2001; 412:202–206. [PubMed: 11449279]
43. Reddien PW, Cameron S, Horvitz HR. Phagocytosis promotes programmed cell death in *C. elegans*. *Nature*. 2001; 412:198–202. [PubMed: 11449278]
44. Church DL, Guan KL, Lambie EJ. Three genes of the MAP kinase cascade, *mek-2*, *mpk-1/sur-1* and *let-60* ras, are required for meiotic cell cycle progression in *Caenorhabditis elegans*. *Development*. 1995; 121:2525–2535. [PubMed: 7671816]
45. Lee MH, Ohmachi M, Arur S, Nayak S, Francis R, Church D, Lambie E, Schedl T. Multiple functions and dynamic activation of MPK-1 extracellular signal-regulated kinase signaling in *Caenorhabditis elegans* germline development. *Genetics*. 2007; 177:2039–2062. [PubMed: 18073423]
46. Zermati Y, Mouhamad S, Stergiou L, Besse B, Galluzzi L, Bohrer S, Pauleau AL, Rosselli F, D’Amelio M, Amendola R, et al. Nonapoptotic role for Apaf-1 in the DNA damage checkpoint. *Mol Cell*. 2007; 28:624–637. [PubMed: 18042457]
47. Lu WJ, Chappo J, Roig I, Abrams JM. Meiotic recombination provokes functional activation of the p53 regulatory network. *Science*. 2010; 328:1278–1281. [PubMed: 20522776]
48. Jelinsky SA, Samson LD. Global response of *Saccharomyces cerevisiae* to an alkylating agent. *Proc Natl Acad Sci U S A*. 1999; 96:1486–1491. [PubMed: 9990050]
49. Dawson DS, Murray AW, Szostak JW. An alternative pathway for meiotic chromosome segregation in yeast. *Science*. 1986; 234:713–717. [PubMed: 3535068]
50. Grell RF. A new hypothesis on the nature and sequence of meiotic events in the female of *Drosophila melanogaster*. *Proc Natl Acad Sci U S A*. 1962; 48:165–172. [PubMed: 13901696]
51. Shakes DC, Wu JC, Sadler PL, Laprade K, Moore LL, Noritake A, Chu DS. Spermatogenesis-specific features of the meiotic program in *Caenorhabditis elegans*. *PLoS Genet*. 2009; 5:e1000611. [PubMed: 19696886]
52. Wignall SM, Villeneuve AM. Lateral microtubule bundles promote chromosome alignment during acentrosomal oocyte meiosis. *Nat Cell Biol*. 2009; 11:839–844. [PubMed: 19525937]
53. Conradt B, Xue D. Programmed cell death. *WormBook*. 2005:1–13. [PubMed: 18061982]



B

Genotype	No. apoptotic germ cells (N)	
	Hermaphrodites	Males
WT	2.5±0.3 (111)	0 (37)
WT + IR	14.0±0.9 (56)	0 (27)
<i>syp-1(me17)</i>	12.0±0.5 (33)	0 (18)
<i>rad-51(RNAi)</i>	5.2±0.7 (36)	0 (13)
<i>chk-1(RNAi)</i>	3.1±0.4 (46)*	ND
<i>chk-1(RNAi) +IR</i>	6.8±1.0 (41)	ND

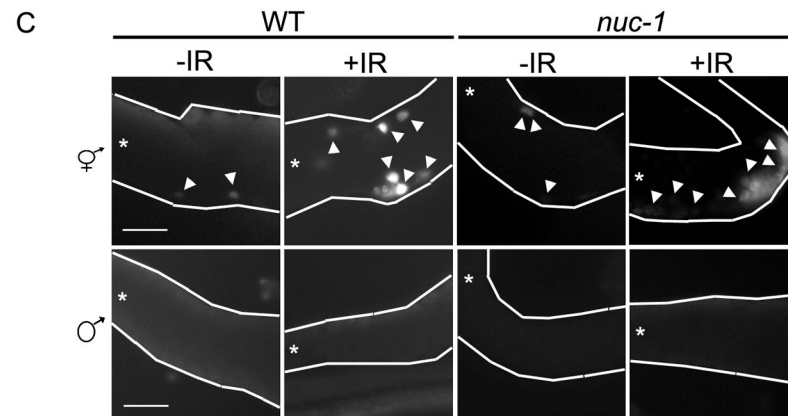


Figure 1. DNA damage, chromosome asynapsis and/or unrepaired meiotic DSBs do not induce apoptosis in the male germ line. (A) Cartoon of hermaphrodite (left) and male (right) germ lines. Distal end is capped by somatic distal tip cell(s) and contains a stem cell population of proliferating germ cells (black). Hermaphrodites produce sperm (small dark grey) during larval stages and then switch to oogenesis as adults. Germ cells move towards the proximal gonad where they enter meiotic prophase in the transition zone (leptotene/zygotene; grey crescents) and then progress through pachytene and diplotene (grey circles). In the proximal gonad germ cells are in diakinesis and are packaged into oocytes (dark grey). Apoptosis occurs during the pachytene stage of oogenesis mainly in the gonad loop region (apoptosis

zone; circled grey cells). In the male gonad, germ cells differentiate into spermatocytes (grey triangles) and then sperm (dark grey circles); no apoptosis occurs. (B) Number of apoptotic nuclei per gonad arm measured by AO staining 24h post L4 stage (and 24 h post IR). The number of germ lines scored for each genotype is in parenthesis. The data shown are means \pm S.E.M. Statistical comparisons between the mutants and wild type were conducted using the two-tailed Mann-Whitney test and all differed significantly ($p < 0.001$) except (*) where $p > 0.05$. (C) TUNEL staining of wild-type and *nuc-1* hermaphrodite and male germ lines in the presence and absence of IR. The gonads are outlined in white and show the pachytene region. All panels oriented with distal to left (*). Arrowheads mark some of the white, TUNEL-positive nuclei. Scale bar, 20 μ m.

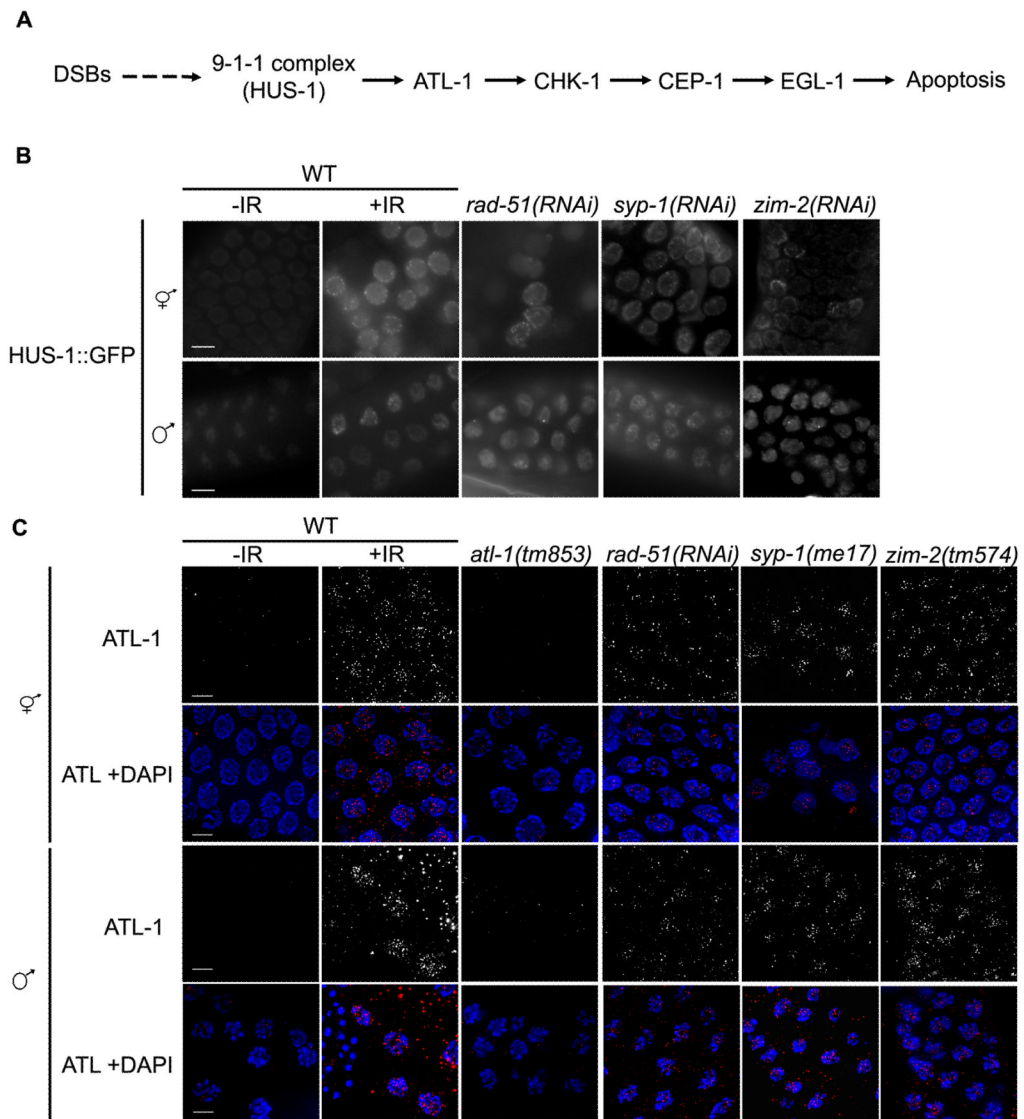
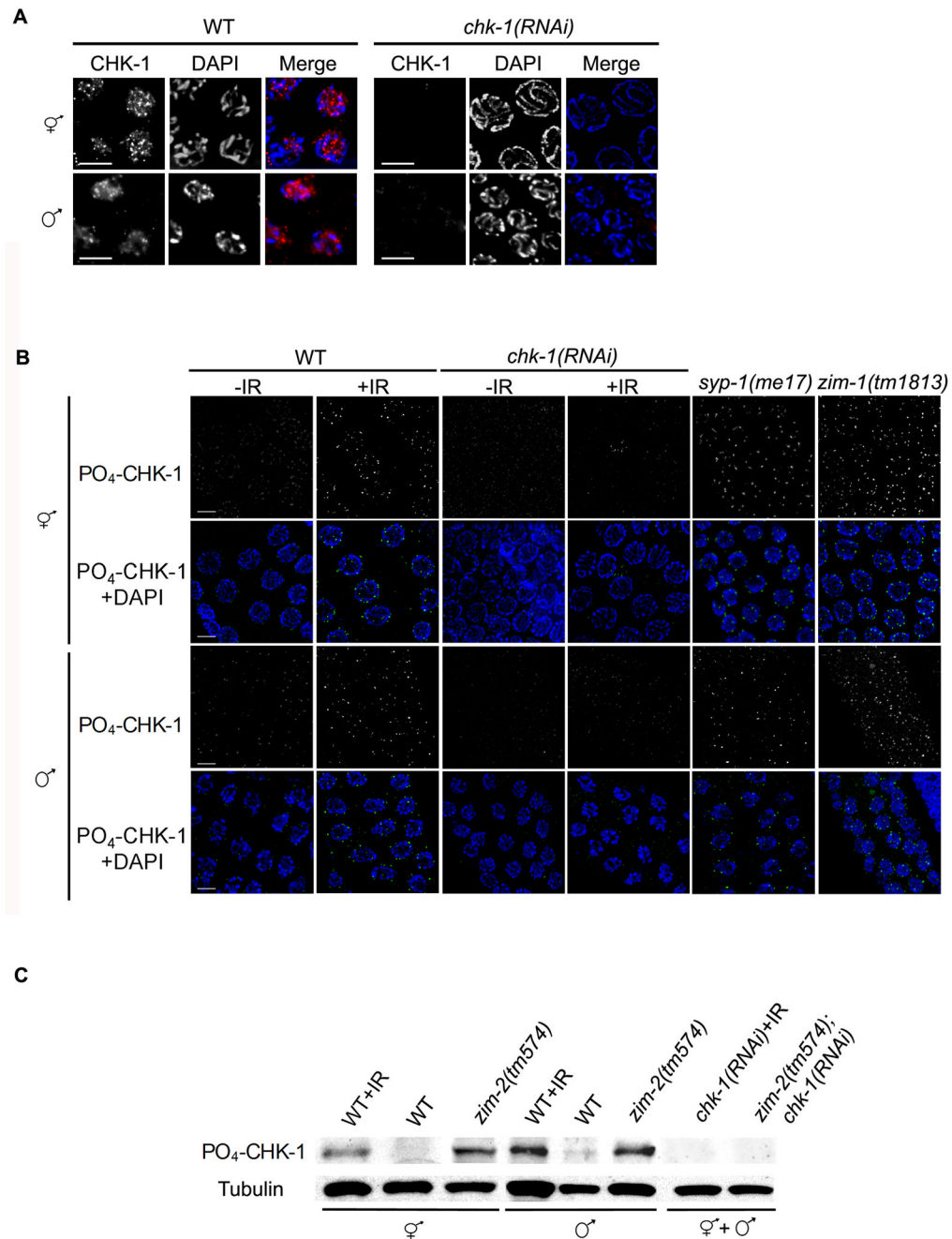
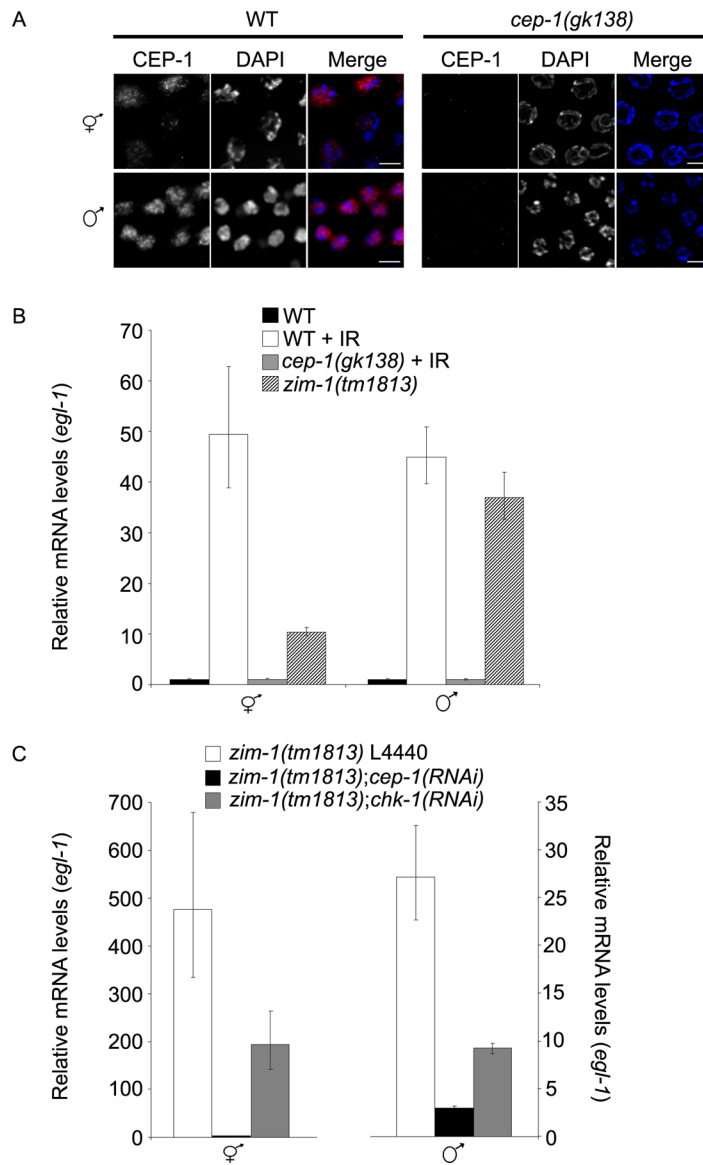


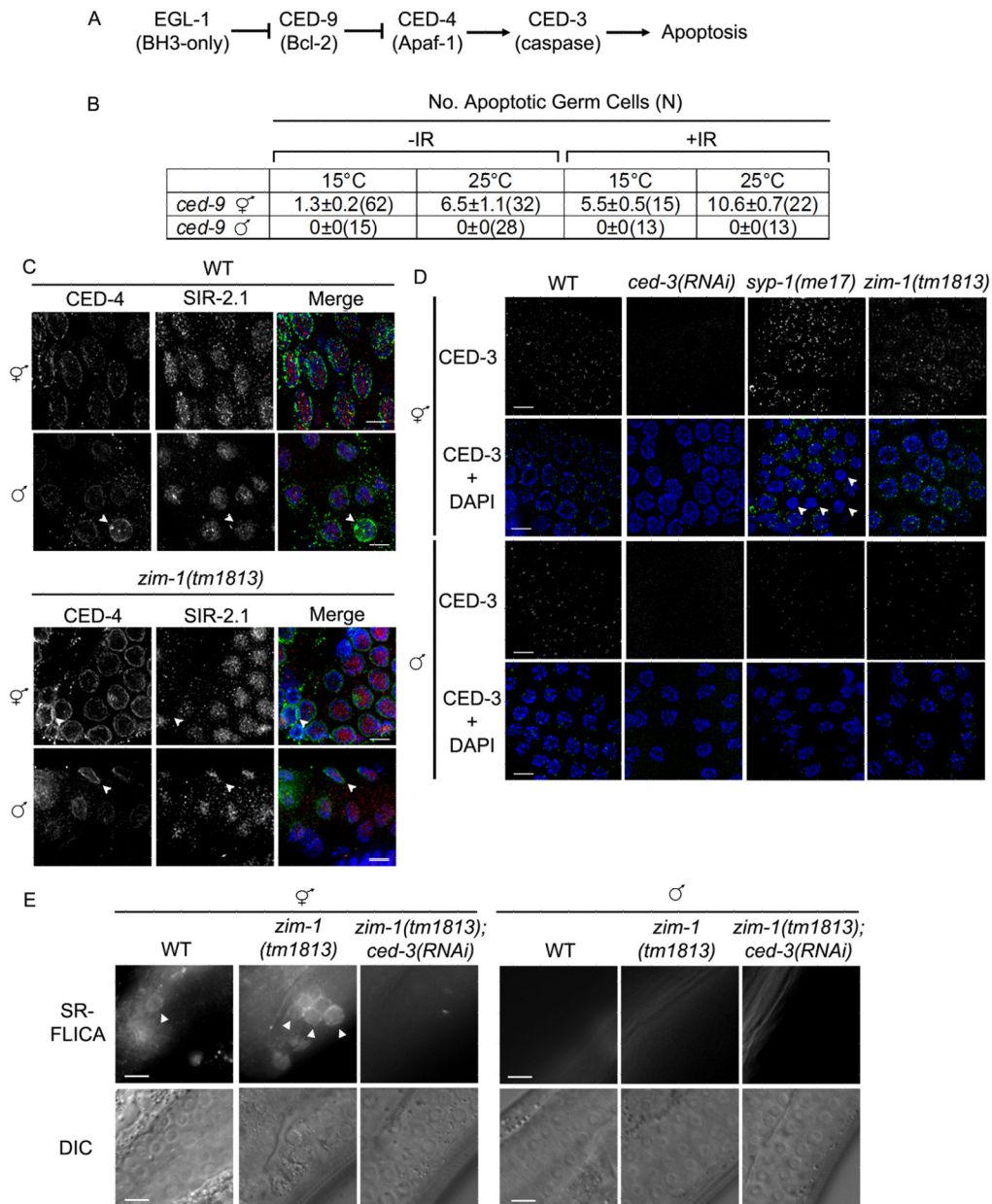
Figure 2. HUS-1::GFP and ATL-1 localize to chromatin following DNA damage, chromosome asynapsis and/or unrepaired meiotic DSBs in hermaphrodite and male germ lines. (A) Checkpoint signaling pathway in response to unrepaired recombination intermediates and IR-induced DSBs (modified from [26]). Scale bars, 5 μ m. (B) Fluorescence microscopy of pachytene nuclei expressing HUS-1::GFP(*opIs34*); both hermaphrodite and male germ cells exhibit HUS1::GFP on chromatin under checkpoint-activating conditions. Young adult worms were examined 8h after irradiation (120 Gy). Mutant and RNAi treated worms were examined 24h post L4. (C) ATL-1 is recruited to chromatin following IR or in meiotic mutants; immunolocalization of ATL-1 in fixed pachytene nuclei of adult worms (24h post L4). Young adult worms were examined 1h after IR treatment (120 Gy). Mutant and RNAi treated worms were examined 24h post L4. Scale bars, 5 μ m.

**Figure 3.**

CHK-1 is expressed and phosphorylated in hermaphrodite and male germ lines. (A) Localization of CHK-1 using antibodies directed against full-length CHK-1 (red) in pachytene nuclei of wild-type and *chk-1(RNAi)* hermaphrodite and male germ lines counterstained with DAPI (blue). Scale bars, 5 μ m. (B) Localization of CHK-1 phosphorylated on Serine 345 (PO₄-CHK-1; green in merge) in fixed pachytene nuclei of young adult worms 6h after IR treatment (120 Gy). Mutant and RNAi treated worms were examined 24h post L4. Scale bars, 5 μ m. (C) Hermaphrodite and male worm extracts analyzed by immunoblotting using antibodies to PO₄-CHK-1 (~60kD), and α -tubulin (~50kD) as loading control.

**Figure 4.**

CEP-1 is expressed and induces EGL-1 transcription in response to DNA damage or unrepaired recombination intermediates in both hermaphrodite and male germ lines. (A) Immunolocalization of CEP-1 (red) counterstained with DAPI (blue) in pachytene nuclei from wild-type and *cep-1(gk138)* hermaphrodite and male germ lines. Scale bars, 5 μ m. (B) *egl-1* transcript levels are induced following DNA damage or in the presence of unrepaired meiotic DSBs in hermaphrodites and males. Relative *egl-1* transcript levels as determined by qRT-PCR following IR and/or in mutant germ lines. RNA was extracted from wild-type and *cep-1* hermaphrodites and males 24h following treatment with IR (120 Gy) and 24h post-L4 for *zim-1* hermaphrodites and males. (C) Transcriptional induction of *egl-1* in *zim-1* hermaphrodite and male germ cells is dependent on *cep-1* and *chk-1*. Relative mRNA levels were determined by qRT-PCR in *zim-1* L4440, *zim-1;cep-1(RNAi)* and *zim-1;chk-1(RNAi)* hermaphrodites (left) and males (right) 24h post-L4. Data shown for B and C are representative of three independent extractions and qRT-PCR reactions; error bars indicate standard deviation of 3 individual replicas of each sample.

**Figure 5.**

The pro-apoptotic machinery is expressed in the male germ line during meiotic prophase, but CED-3 caspase is not activated. (A) Pathway of germ cell apoptosis in *C. elegans* [53]. (B) CED-9 inactivation does not induce apoptosis in the male germ line. Number of apoptotic nuclei per gonad arm measured by AO staining 24h post L4 stage (and 24h post IR). The number of germ lines scored for each genotype is in parenthesis. The data shown are means ± S.E.M. (C) CED-4 and SIR-2.1 are expressed in both hermaphrodite and male germ lines but no SIR-2.1 translocation occurs in male germ cells. Immunolocalization of CED-4 (green) and SIR-2.1 (red) counterstained with DAPI (blue) in pachytene nuclei from wild-type and *zim-1(tm1813)* hermaphrodite and male germ lines. Arrowheads point to nuclei with more intense CED-4 staining. Scale bars, 5µm. (D) CED-3 is expressed in hermaphrodite and male germ lines but levels do not increase under checkpoint-activating conditions in the male germ line. CED-3 immunolocalization (green) in pachytene nuclei

stained with DAPI (blue) of adult worms (24h post L4). Arrowheads indicate apoptotic nuclei that lack CED-3 staining presumably because they have proceeded to a later stage. Scale bars, 5 μ m. (E) Males do not activate CED-3 caspase. Caspase activity was monitored by fluorescence microscopy following microinjection of SR-FLICA inhibitor in hermaphrodite and male germ lines of N2, *zim-1(tm1813)* and *zim-1(tm1813);ced-3(RNAi)* worms. Arrowheads mark some of the caspase-positive cells. Scale bars, 10 μ m.

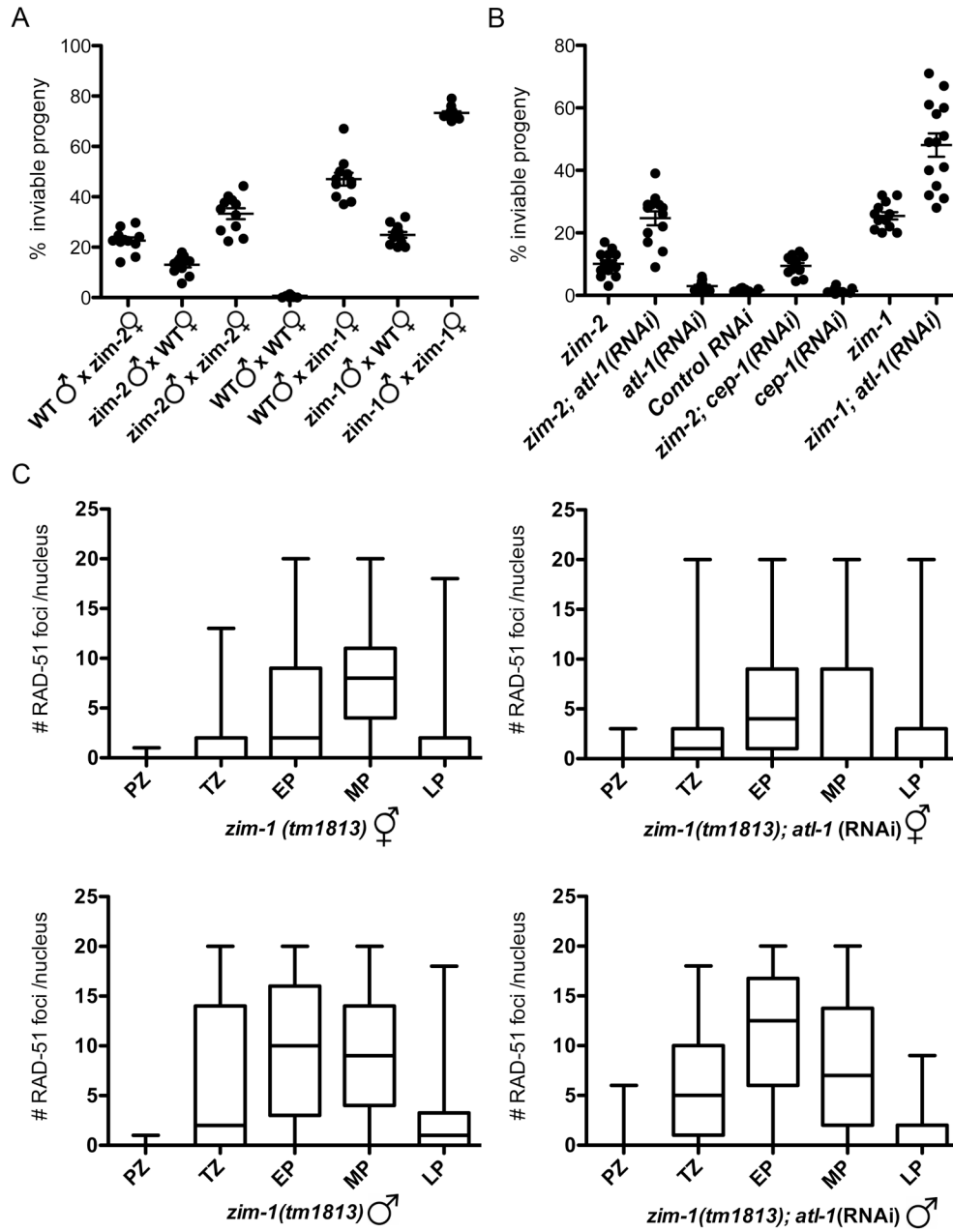


Figure 6.

The recombination checkpoint functions in the male germline to enhance gamete quality when meiosis is impaired. (A) Progeny sired by *zim-2(tm574)* or *zim-1(tm1813)* males have better viability than progeny derived from *zim-2(tm574)* or *zim-1(tm1813)* females. Percentage of inviable progeny from indicated crosses using *fog-2(q71)* females. Each point represents an individual mating; a minimum of 11 matings was analyzed for each genotype. Progeny inviability from crosses of WT males x *zim-2* females compared to *zim-2* males x WT females ($p < 0.0005$) and WT males x *zim-1* females compared to *zim-1* males x WT females differed significantly ($p < 0.0001$) using the Mann-Whitney test. Brood sizes: WT = 417 ± 25 ; WT males X *zim-2* females = 312 ± 27 ; *zim-2* males x WT females = 452 ± 37 ; *zim-2* = 303 ± 45 ; WT males x *zim-1* females = 253 ± 33 ; *zim-1* males x WT females = 362 ± 24 ; *zim-1* = 214 ± 17 (means \pm S.E.M.). (B) Depletion of ATL-1 results in reduced viability of

progeny sired by *zim-2(tm574)* and *zim-1(tm1813)* males. Percentage of inviable progeny from crosses of indicated males to *fog-2(q71)* females. 12 matings were analyzed for each genotype. Progeny inviability from crosses of *zim-2* males compared to *zim-2;atl-1(RNAi)* males ($p<0.0005$) and *zim-1* males compared to *zim-1; atl-1(RNAi)* males ($p<0.0001$) differed significantly using the Mann-Whitney test. Brood sizes: *zim-2; atl-1(RNAi)* males = 347 ± 19 ; *atl-1(RNAi)* males = 340 ± 16 ; *zim-2 cep-1(RNAi)* = 342 ± 19 ; *cep-1(RNAi)* = 358 ± 15 ; *zim-1; atl-1(RNAi)* = 390 ± 19 . (C) Assembly and removal of RAD-51 foci during meiotic prophase progression. Quantification of RAD-51 focus formation in *zim-1(tm1813)* and *zim-1(tm1813); atl-1(RNAi)* hermaphrodites and males. Gonads were divided into prophase substages and nuclei assigned to each region on the basis of morphology and location. Graphs display box-whisker plots of focus numbers. X-axis indicates meiotic prophase stages: Proliferative zone (PZ), transition zone (TZ), early pachytene (EP), mid-pachytene (MP), and late pachytene (LP); y-axis indicates number of RAD-51 foci/nucleus. Center horizontal line of each box indicates the median measurements; lines extending above and below boxes indicate standard deviation. Numbers of nuclei observed for *zim-1(tm1813)* hermaphrodites = 815; *zim-1(tm1813);atl-1(RNAi)* hermaphrodites = 1310; *zim-1(tm1813)* males = 1052; *zim-1(tm1813);atl-1(RNAi)* males = 761.